POLITECNICO DI TORINO
Repository ISTITUZIONALE

Ultrasonic spray freeze-drying of sucrose and mannitol-based formulations: impact of the atomization conditions on the particle morphology and drying performance

(Article begins on next page)

02 December 2024

Ultrasonic spray freeze-drying of sucrose and mannitol-based formulations: impact of the atomization conditions on the particle morphology and drying performance

Merve B. Adali[a], Antonello Barresi[a], Gianluca Boccardo[a], Giorgia Montalbano[a] and Roberto Pisano[a*]

[a]Department of Applied Science and Technology, Politecnico di Torino, Torino, Italy

*E-mail of the corresponding author: roberto.pisano@polito.it

Abstract

Spray freeze-drying is an emerging manufacturing technology that offers many advantages, including long-term stability, consistent particle size distribution, and enhanced bioavailability. However, its implementation on an industrial scale is still hampered by several technical problems relating to the design of the equipment and the selection of appropriate operating conditions. This study aims to clarify the relationship between the atomization conditions (atomizing power, feed flow rate, and viscosity) and the characteristics of the lyophilized powder (particle size distribution and morphology) for two model products (sucrose- and mannitol-based formulations). Independently of the formulation, the particle morphology only depended on its solid content, while the average particle size increased with the feed flow rate and viscosity. Lastly, the specific surface area of the lyophilized powder varied with the initial solid content and the type of excipient as well, with mannitol-based particles having the highest specific surface area.

Keywords: spray freeze-drying; freeze-drying; ultrasonic atomizer; particle morphology; particle size distribution; porous particles

Introduction

Drying is an important unit operation in the pharmaceutical and chemical industries to convert labile liquid formulations into a stable solid-state.[1,2] Freeze-drying has become the most common technique for drying a wide range of materials from food to

biological products and pharmaceuticals, as it is based on the phenomenon of sublimation at low temperature.[3] However, freeze-drying is a highly energy-intensive and economically expensive batch process with a long processing time.[4] The continuous growth in the need for freeze-dried products has resulted in increased energy costs, leading to market efforts to shorten freeze-drying cycles and optimize production.[5,6] Focusing on the pharmaceutical industry, gradually shifting from batch process towards continuous manufacturing has been increased to implement time- and cost-reducing strategies in the last years.[7,8] Scalability from laboratory to production scale is complex and requires the design of the process with the ultimate goal of making a commercially viable product.[9,10] Regulatory agencies also drive production toward continuous manufacturing with an emphasis on quality by design (QbD) and process analytical technology (PAT).[11] Although spray drying is a continuous process with low operating cost and shorter processing time, and the formulation can be optimized by employing QbD and PAT principles, it is a relatively harsh process for heat sensitive materials.[12,13]

Spray freeze-drying (SFD) could be a promising technique for the continuous manufacturing of this class of products.[14] This concept starts with the atomization of a liquid (solution, suspension, or emulsion) into fine droplets which are frozen instantaneously by a cold atmosphere or upon contact with a cryogenic liquid. Subsequently, the solvent is removed from the frozen droplets by sublimation, leading to the formation of porous spherical particles with a large specific surface area.[15-17] There are different SFD approaches distinguished by spray freezing method, spraying in a cold gas stream or spraying in a cryogenic medium. Spray freezing into liquid (SFL), was presented as a micronization procedure for active pharmaceutical ingredients (API) in a patent registered in 2005 by Williams III et al.[18], and commercialized by The Dow

Chemical Company, and later Enavail LLC.[19] SFL involves the atomization of the liquid solution directly into liquid nitrogen through an insulated nozzle. Compared to other liquid cryogens, nitrogen is the most widely used as it is relatively inexpensive, safe, and is already accepted for use in some medical applications.[20] For example, a fully automated process using liquid nitrogen with API has been developed by Teva Pharmaceuticals Industries, where the bulk API is pelleted by dripping into liquid nitrogen to form immediately frozen pellets.[21] Generally, the most employed SFD approach in pharmaceutical applications is the spray freezing into vapor over liquid (SFV/L)[22], where the feed is atomized into the headspace of a container containing the cryogenic medium, so the droplets start freezing during their passage through the cold vapor phase and are collected in the liquid cryogen as frozen particles. SFV/L method shares the same atomization configurations/conditions as spray freezing into vapor (SFV) in some industrial systems where the solution is atomized and frozen into the cold gas stream. Additionally, SFD is an advanced particle engineering technique that enables to control of particle size, morphology, crystallinity, and surface texture/area of dry powders a wide range of therapeutic molecules.[23] A deeper understanding of pharmaceutical particle and powder characterization and its link to advances in production technologies are key to cover the demand for a continuous process of the pharmaceutical industry. Transitioning to continuous manufacturing could allow for careful control of particle properties (particle size, bulk density, etc.) and formulation options from simple to complex besides higher yields, cost-effectiveness, and consistent production.[24] From a processing point of view, generating particle-based drugs to be dried allows reducing the operating costs by saving the drying time. Besides, the freezing step occurs quickly because of atomization due to the increased surface area of the product. Atomization of the liquid is a critical step of SFD

as it is what mostly influences the droplet size and, thus, the particle size distribution of the lyophilized powder.[15,22] This is because the subsequent rapid freezing and freeze-drying processes do not significantly change the size of the droplet once the liquid is atomized.[16] In the case of ultrasonic atomization, the produced droplets have the advantages of having a relatively uniform size distribution[25] and sphericity because of the non-clogging probe of the atomizer[26] and being efficiently captured in liquid nitrogen due to the absence of additional air flow[27-29] that is present in conventional nozzles. Also, the ultrasonic atomizer ensures successful operation at low flow rates. Several studies concerning ultrasonic spray freeze-drying have been performed using a model drug-product for the evaluation of pharmacokinetic characteristics (e.g., dissolution, aerodynamic performance) and drug product quality (e.g., stability, drug release), as reported for example for clarithromycin[30], small nucleic acids[31], colistin and ivacaftor[32]. However, it has not yet been clarified how the frozen particle properties affect the drying performance during freeze-drying. Furthermore, this investigation aimed at examining how operating parameters and liquid characteristics impact the average size and distribution of particles produced by SFD. Sucrose and mannitol were chosen because they are widely used as an excipient in the freeze-drying process. The processing parameters affecting the particle characteristics were investigated by changing the flow rate and concentration of the sugar-based formulation and the final SFD powders were assessed with respect to morphology, particle size, specific surface area, and moisture content.

Materials and methods

Materials

Aqueous solutions containing 5% mannitol, 5% and 40% (w/w) sucrose (Sigma-Aldrich-Fluka, Buchs, Switzerland) were prepared by dissolving either mannitol or sucrose in water for injection (Fresenius Kabi, Verona, Italy).

The glass transition temperatures of solutions (Tg') were determined using a differential scanning calorimeter (DSC type Q200, TA Instruments, New Castle, DE, USA). Approximately 30 µL of each solution was placed into an aluminium pan, which was hermetically sealed. The samples were cooled down to −80 ºC at 10 °C/min and, then, heated to 20 °C at a rate of 1.5 °C/min. The results were subsequently evaluated by using Universal Analysis software (TA Instruments).

Spray freeze-drying

As illustrated in Figure 1, the liquid solution was fed via a digitally controlled syringe pump (Model KDS 200, KD Scientific, Holliston, MA) at 1-10 mL/min into an ultrasonic nozzle (60-kHz atomizing frequency, Buchi, Switzerland) operated at 3W. The atomizing nozzle was positioned 7-10 cm above the liquid nitrogen to spray the solutions into vapor over liquid nitrogen in a Dewar. The atomized droplets fell by gravity, settled into the liquid nitrogen, and were dispersed using a magnetic stirrer. After the spraying of the solution was complete, most of the liquid nitrogen was evaporated, and the frozen droplets were collected and transferred to the freeze-dryer (Revo, Millrock Technology, Kingston, NY) with precooled shelves at -50 °C. Primary drying was performed at 10 °C and 20 Pa for mannitol, and -20 °C and 10 Pa in the case of sucrose. The pressure within the chamber was monitored using both a Pirani and a

capacitance (MKS Baratron) manometer, and the end of primary drying was determined by the Pirani/Baratron ratio.[33] For both types of formulations, secondary drying was conducted at 20 °C for 5 h. The dried powders were then collected from the tray under nitrogen purge and stored at -20 °C until use.

Scanning electron microscopy (SEM) and the particle size determination

The average size and morphology of spray freeze-dried particles were examined using a Desktop SEM Phenom XL (Phenom-World B.V., Netherlands) at an accelerating voltage of 15 kV and different magnifications. A small amount of powder was deposited on top of double-sided carbon tape on an aluminium holder (3.05 mm, TAAB, Aldermaston, Berks, UK). The particles were then coated with 8nm platinum using a sputter coater (Balzer AG, type 120B, Balzers, Liechtenstein) before imaging.

To determine the geometric diameter of dry particles, SEM images were analyzed using the software ImageJ (NIH, USA), and 200-300 particles were measured for each sample. An automatic determination of the particle size distribution by image analysis was not possible due to overlapping particles. The average particle size in μm was calculated manually with the ImageJ tools *straight selection* and *oval selection.*

Particle size distributions were also characterized by their span using the cumulative frequency distribution, and the span value was calculated according to the equation of (D90-D10)/D50, where D90, D10, and D50 represent the diameters at 90%, 10%, and 50% cumulative percent undersize.

Specific surface area

The specific surface area (SSA) of the prepared powders was calculated using the model of Brunauer, Emmett, and Teller (BET) using a Micromeritics ASAP 2020

(Micromeritics, USA) apparatus. Approximately 200 mg of powder was loaded into the glass BET sample cell and then degassed at 40 °C for 3 h before analysis. Nitrogen adsorption-desorption isotherms were measured at the temperature of 77 K over a relative pressure (P/P_0) range of 0.05–0.30.

Powder X-ray diffraction

For mannitol powders, X-ray diffractometry was also conducted to identify their polymorphic state. X-ray diffraction (XRD) patterns were characterized using Cu-Kα radiation with a wavelength of 1.54054 Å at 40 kV and 40 mA from an X-ray diffractometer (XRD, X-pert Powder type, PANalytical, Almelo, Netherlands). The sample powder was placed in a sample holder and scanned from 5 to 65° (2θ) range at each 0.026°.

Karl–Fischer titration analysis

Residual moisture in the powders was measured using the automated Karl Fischer titration (KF Coulometer type DL32, Mettler Toledo, Novate Milanese, Italy). Approximately 50–100 mg of powder was dissolved in 2-3 mL of Karl Fischer reagent and then, injected into the Karl Fischer titrator cell to react with the titration reagent under magnetic stirring. The water content of the sample was calculated with reference to the dried weight of the sample.

Results and discussion

Thermal properties of solutions

The thermal behavior of the three formulations was investigated by DSC, and the thermograms obtained are presented in Figure 2. The Tg' values of sucrose solutions

were clearly detectable and were found to be -32.39 °C and -33.26 °C for 5% and 40% (w/w) sucrose solution respectively, which agree with those reported in the literature.[34-36] The Tg' value differed only slightly; it was observed that a higher initial concentration caused a more pronounced change in heat capacity at Tg'. The Tg' of 5% (w/w) mannitol solution was immediately followed by the exothermic crystallization peak starting at -26 °C. As reported in the literature, the glass transition temperature of the maximally freeze-concentrated mannitol is around -30 °C.[37,38] These results were a guide for selecting a safe freeze-drying process temperature range for the solutions being processed in the SFD to prevent particles from collapsing or melting.

Influence of the atomization conditions and feed solution characteristics on the spray freeze-dried particle morphology

The particle morphology

Figure 3 shows the shape and morphology of the mannitol and sucrose-based particles examined by SEM. All particles had high-porous structures which are expected from a theoretical point of view as fast freezing of the sprayed droplets results in the formation of smaller ice crystals, which on subsequent sublimation during the primary phase of the freeze-drying step resulted in a porous surface. However, a structural difference was noticeable in the particles as the concentration increased. The surface of the particles obtained from 5% (w/w) mannitol and 5% (w/w) sucrose solution had a larger porous and rough appearance compared to the particles generated from 40% (w/w) sucrose solution (Figure 3). The particles with a higher sucrose concentration formed a more compact surface with smaller pore size. This may be due to the high solute content in the droplets interrupting the growth of ice crystals during the freezing process, which also reveals the formation of many small pores on the particles produced, according to

the qualitative evaluation of SEM images. Furthermore, the increase in the solid content of the spray solution leads to high-density particles, which can trigger particle shrinkage. Besides the changes in surface morphology, Figure 3 shows that the particle shape also changed with increasing concentration in the case of sucrose-based formulation and increasing flow rates in the case of mannitol formulation.

Figure 4 shows that for 5% (w/w) mannitol, particle shape and morphology were dramatically affected by varying the feed flow rate. The resulting spherical particles were porous and fragile enough to cause them to collapse easily during handling. The particles sprayed in the range of 2.5 to 7.5 mL/min were spherical with an enormous number of pores on both the surface and the inside (Figure 4), whereas at 1 and 10 mL/min the spherical particles lost their shape and appeared to be fragmented mostly into a sponge-like structure (Figure 3 and 4).

Figures 5 and 6 show that, in the case of the sucrose-based formulation, the change in the feed flow rate did not significantly affect the shape and morphology of the particles at a concentration of either 5% (Figure 5) or 40% (w/w) (Figure 6). Independently of the feed flow rate, the 5% sucrose-based particles showed a highly porous spherical shape, while the 40% (w/w) sucrose-based ones showed a rough and wrinkled surface while the pores remained. However, the size of pores observed in the 40% (w/w) sucrose particles was much smaller than those of 5% (w/w) sucrose particles (Figure 4).

As mentioned above, in the case of sucrose-based formulation, raising the concentration from 5% to 40% (w/w), thus the viscosity from 1.11 to 6.14 mPa s[39], resulted in noticeable shape and morphology differences. As shown in Figure 5, the particles produced for a concentration of 5% (w/w) sucrose resulted in small spherical and very cohesive agglomerates compared to the relatively larger particles prepared

from a high concentration sucrose solution of 40% (w/w) (Figure 6). At a concentration of 40% (w/w) sucrose, although nearly perfect spherical particles with a smooth surface were produced, most of the particles shrank and showed several indentations on the particle surface (Figure 6).

The particle size distribution

Figures 4, 5, and 6 show the particle size distribution for the 5% mannitol, 5% and 40% (w/w) sucrose-based samples. The feed flow rate and concentration have been shown to affect the average particle size in the resulting powders.

From Table 1, it can be inferred that the average particle size increased as the feed flow rate increased. This trend is true for all the three formulations here investigated. The average diameter of 5% (w/w) mannitol particles (14.99 – 65.96 µm). Although most of the 5% (w/w) mannitol particles were hidden because of spongy-like structure (Figure 4), the particles sprayed at 1 mL/min were small with an average diameter of 14.99 µm, while the particles at 10 mL/min yielded an average diameter of 65.96 µm. These particles were similar in size to the mannitol particles found in the literature, which were produced using a 40 kHz ultrasonic atomizer at a flow rate of 0.5 mL/min.[27] In the case of 5% (w/w) sucrose particles, the average diameter ranged from 14.55 µm to 30.36 µm. Using a flow rate of 10 mL/min, 5% (w/w) sucrose particles yielded particles yielded 30.36 µm in size, i.e., three times smaller than mannitol particles obtained at 10 mL/min. Therefore, it can be noted that 5% (w/w) sucrose particles demonstrated a smaller variation in size distributions compared to the 5% (w/w) mannitol particles. A relatively narrow range was also observed for the 40% (w/w) sucrose particles in the range of 30.90 to 47.63 µm (Table 1). It should be noted that there is a relationship between the atomizer frequency and the flow rate, which

affects the particle size distribution. The ratio of volumetric flow rate to frequency can express the average volume per drop that indicates particle size. The latter means, similar particle size could be obtained from a similar ratio of volumetric flow rate to frequency. In addition, the thickness of a thin film formed on the vibrating surface of the ultrasonic atomizer also influences the droplet size, which can be controlled by adjusting the liquid flow rate. The results demonstrated that the droplet size increased with an increase in the flow rate (Table 1), which contributed to an increase in the thickness of the liquid film on the vibrating surface before atomization. It is known that liquid film thickness is affected by the natural characteristics of the liquid, mainly its viscosity and surface tension.

Table 1 shows the effect of the sucrose concentration on the average particle size. Increasing the concentration from 5% to 40% (w/w), thus the viscosity, the average particle size increased from 14.55 to 30.90 µm at 1 mL/min, and 30.36 to 47.63 µm in the case of 10 mL/min. This increase in the average particle size could be attributed to the increased viscosity of the solution as the solid content increased.[40-42] Similarly, a two-order increase in solution viscosity appeared to be the cause of a 20% change in median droplet size, assuming the effect of film thickness occurring at the atomizer tip.[42]

The specific surface area

Table 1 shows that the specific surface area of mannitol and sucrose powders obtained by spraying at different feed flow rates varied between 0.23 and 8.97 m²/g.

The specific surface area increased with increasing solution concentration. As shown in Table 1, the lowest specific surface area (0.23 m²/g) was obtained in particles prepared from the 5% (w/w) sucrose at 1 mL/min, which was six times smaller than

those observed for 40% (w/w) sucrose. Likewise, the highest value (8.97 m²/g) was determined in the more concentrated formulation of sucrose at 10 mL/min, which was four times bigger than those of the dilute formulation of sucrose at the same flow rate. From the morphological point of view (Figure 3), although the particles prepared from 5% (w/w) sucrose appeared to have a higher specific surface area than those obtained from 40% (w/w) sucrose, the specific surface area data showed the opposite results. In other words, 40% (w/w) of sucrose particles with a smooth surface have many pores in very small sizes on the surface and inside the particles. This observation was similar to that reported by studies involving the use of a two-fluid nozzle for particle production, resulting in increased specific surface area and mean particle size as the amount of tolbutamide increased.[44,45] Due to the crystallization of the excipients, the size of the pores decreases as the concentration increases, where the higher concentration results in more freeze concentration and more inhibition of crystal growth, thus smaller crystal sizes. The specific surface area also increased with increasing flow rates in the case of both sucrose-based formulations (Table 1). Indeed, contrary to expectations, an inverse relationship between the average particle size and the specific surface area was found. However, no correlation was found between the average particle size and the specific surface area for the particles obtained from 5% (w/w) mannitol solution at different flow rates (Table 1). They all exhibited a very similar specific surface area with respect to their particle size. This behavior could be due to the particle internal porosity because the gas adsorption-based BET measurements include not only the external but also the internal specific surface area of the particles. For mannitol particles, the specific surface area due to internal porosity was considerably larger than that due to external porosity, hence the size of the particle. That is why there was no relation between the particle size of mannitol and its specific surface area. It is also supposed that changing atomizing

conditions, mannitol can form different polymorphs or the same polymorphs but with different compositions. Since the various polymorphs show significantly different specific surface area, these differences could cover the relationship between the average particle size and specific surface area.

X-ray powder diffraction

Figure 7 illustrates the crystallinity of mannitol powders examined by XRD. All the mannitol powders shared highly similar XRD profiles, suggesting that the changing of flow rates did not alter the polymorph composition of mannitol. The intense diffraction peaks, which appeared in the mannitol powders at around 9.7° and 18.7°, indicate the presence of δ and β forms, respectively. The intensity of these peaks was not influenced when the liquid flow rate was increased. The presence of mannitol hemihydrate form was confirmed because of the presence of its characteristic peaks at 16.5° in the assayed samples, whereas no clear peak for the α form was detected. It must also be noted that the freezing rate of mannitol solutions also affects the crystallization behavior: as it was shown in other studies of mannitol freeze-drying[22,46], slow freezing of solutions resulted in a mixture of α and β polymorphs, while rapid freezing, which is the case of SFD, primarily produced δ polymorph.[37]

Drying behavior and water content of the SFD powders

For all the three formulations investigated, the frozen particles produced at 1 and 10 mL/min were lyophilized with the packed-bed heights of 3 mm. Figure 8 compares the primary drying time as observed for the three formulations. More specifically, the onset and offset time were determined based on the pressure ratio signal between Pirani and Baratron.[33] As well known in the literature, the onset point corresponds to the time when the Pirani gauge begins to decay, which indicates that the ice sublimation is

completed in a large fraction of the batch. On the other hand, the offset shows the point at which the ratio of Pirani and Baratron is equal to 1, meaning that the ice sublimation is complete within the entire batch. The offset time was 5 h and 6 h for 5% (w/w) mannitol and 5% (w/w) sucrose, respectively, considering the offset values of both flow rates being processed. Nevertheless, in the case of 40% (w/w) sucrose, the offset value was found at 6.5 h for the flow rate of 1 mL/min and 8 h for the flow rate of 10 mL/min. The solid content of liquid seems to influence drying time, there is a difference between drying times of 5% (w/w) sucrose for 6 h and 40% (w/w) sucrose for 8 h, which demonstrates SFD can be highly beneficial when using solid concentrations typical of pharmaceutical formulations (5-10%). It has been stated that the aerosol performance of the SFD powders also depends on the solution concentration. As the solute concentration increases, the fine particle fraction (FPF), the parameter indicating the fraction of powder with an aerodynamic diameter <5 µm, gradually decreases, hence aerosol performance degrades. For example, the mannitol/DNA powder prepared from the less concentrated 5% (w/v) formulation exhibited a significantly higher FPF (20%) compared to those prepared from a formulation of 7.5% (w/v) solute concentration (FPF 15%).[31] It should also be noted that the difference between onset and offset time is a good indicator of batch uniformity. A large onset and offset time difference mean that the sublimation rate varies within the batch as a result of product heterogeneity. In the case of 40% (w/w) sucrose powder, it was found that the difference between onset and offset time was slightly higher with respect to 5% (w/w) mannitol and sucrose powder, meaning that heterogeneity in the packed bed of particles increased with increasing solid concentration. In addition, the particle size distribution of 40% (w/w) sucrose was wider than that of 5% (w/w) mannitol and sucrose, which also contributed to the heterogeneity of the packed bed.

Table 1 presents the moisture content of each spray freeze-dried powders at various flow rates after a lyophilization involving 5 h secondary drying at 20 °C. As it was reasonably expected, it has been shown that powders obtained from sucrose solution have higher moisture content than those obtained from mannitol solution, since amorphous products retain more water than crystalline products. At a flow rate of 1 mL/min, the moisture content of 5% (w/w) sucrose powder was 5.92 ± 0.09% and it slightly decreased to 3.99 ± 0.13% at 10 mL/min, while it was in the ranged of 6% for the other flow rates (Table 1). In the case of 40% (w/w) sucrose powders, the lowest moisture content was 3.30 ± 0.11% at 7.5 mL/min flow rate, while the highest was 4.91 ± 0.58% at 10 mL/min flow rate. It could be explained by the fact that the larger specific surface area of the particles from 40% (w/w) sucrose results in easier water desorption due to more water molecules being exposed to evaporation and escaping from the water surface. The increased specific surface area with a higher number of smaller pores enhanced the desorption rate during secondary drying and resulted in lower moisture content for 40% (w/w) sucrose powders. The same trend was also found to be associated with the increase in flow rates. For both 5% and 40% sucrose solutions, the moisture contents decreased as the flow rates increased because the kinetics constant of desorption might have been enhanced during secondary drying due to the larger specific surface area. 5% (w/w) mannitol powders had lower moisture content than those observed for the sucrose-based formulations, in the range of 0.94 ± 0.10% and 1.81 ± 0.24%. It is a well-known fact that a longer secondary drying process and/or a higher shelf temperature during secondary drying could reduce the residual water content to a lower value if needed.

Powder stickiness, which can cause agglomeration and clumping of particles, is another concern related to particle quality as well as drying condition, collecting, and

packaging. Amorphous sucrose is known to be hygroscopic in the solid state and exhibits powder stickiness with further moisture absorption. The reduction in the particle size increases the cohesion of the particle, hygroscopicity and the stickiness of the powder. While the powders with 5% (w/w) sucrose solution displayed a cohesive rather than sticky structure, free-flowing powders were obtained for a 40% (w/w) sucrose solution with low moisture content. The poor flowing behavior of the SFD powders attributed to small particles, which leads to aggregation.[30,47]

Conclusions

The implementation of innovative continuous manufacturing requires a precise definition of the acceptable range for all product and process parameters that ensure the critical quality characteristics of the final product are met. Spray freeze-drying as an emerging concept, which makes continuous manufacturing possible, was employed in this study to produce particles of mannitol- and sucrose-based formulations. This study demonstrated that the use of variation in process parameters (atomizing power, feed flow rate, and viscosity) modifies the characteristics of the final particle. The ultrasonic atomizer used in this study produced particles with an average diameter in the range of 14.55 to 65.96 µm. A ten-fold increase in the flow rate led to a two- to three-fold increase in particle size. Moreover, increasing the concentration of sucrose from 5% to 40% (w/w) in the liquid solution resulted in increased particle size. The 5% (w/w) mannitol powders exhibited high specific surface areas for all investigated flow rates in the range of 5.55 to 7.58 m^2/g. Also, we observed differences in drying time between mannitol and sucrose-based powders which were related to variations in the morphology and particle size, even if this phenomenon worth to be further analyzed.

Acknowledgments

References

[1]   Pikal, M. J. Freeze Drying. *Encyclopedia of pharmaceutical technology*; Informa Healthcare: USA, New York, 2007, 1807.

[2]   Costantino, H. R.; Pikal, M. J. *Lyophilization of biopharmaceuticals*; AAPS Press: Arlington, Virginia, 2004.

[3]   Rey, L.; May, J. C. *Freeze drying/lyophilization of pharmaceutical and biological products*; Informa Healthcare: New York, 2010.

[4]   Mortier, S. T. F. C.; Van Bockstal, P. J.; Corver, J.; Nopens, I.; Gernaey, K. V.; De Beer, T. Uncertainty Analysis as Essential Step in the Establishment of the Dynamic Design Space of Primary Drying during Freeze-Drying. *Eur. J. Pharm. Biopharm.* **2016,** *103*, 71–83.

[5]   Tang, X.; Pikal, M. J. Design of Freeze-Drying Processes for Pharmaceuticals: Practical Advice. *Pharm. Res.* **2004,** *21* (2), 191–200.

[6]   Stratta, L.; Capozzi, L. C.; Franzino, S.; Pisano, R. Economic Analysis of a Freeze-Drying Cycle. *Processes* **2020,** *8* (11), 1–17.

[7]   Pisano, R.; Arsiccio, A.; Capozzi, L. C.; Trout, B. L. Achieving Continuous Manufacturing in Lyophilization: Technologies and Approaches. *Eur. J. Pharm. Biopharm.* **2019,** *142*, 265-279.

[8]   U.S. Food and Drug Administration (FDA). Quality considerations for continuous manufacturing guidance for industry draft guidance. Ind Draft Guid. **2019,** 1-27. https://www.fda.gov/Drugs/GuidanceComplianceRegulatoryInformation/Guidances/default.htm (accessed May 9, 2021).

[9]   Arsiccio, A.; Barresi, A.; De Beer, T.; Oddone, I.; Van Bockstal, P. J.; Pisano, R. Vacuum Induced Surface Freezing as an Effective Method for Improved Inter- and Intra-Vial Product Homogeneity. *Eur. J. Pharm. Biopharm.* **2018,** *128*, 210-219.

[10]   Harguindeguy, M.; Fissore, D. Micro Freeze-Dryer and Infrared-Based PAT: Novel Tools for Primary Drying Design Space Determination of Freeze-Drying Processes. *Pharm. Res.* **2021,** *38*, 707-719.

[11] U.S. Food and Drug Administration (FDA). Guidance for Industry, PAT-A Framework for innovative pharmaceutical development, manufacturing and quality assurance. **2004,**. http://www.fda.gov/downloads/Drugs/GuidanceComplianceRegulatoryInformation/Guidances/ucm070305.pdf (accessed May 9, 2021).

[12] Zhang, L.; Mao, S. Application of Quality by Design in the Current Drug Development. *Asian J. Pharm. Sci.*, **2017,** *12*(1), 1–8.

[13] Poozesh, S.; Bilgili, E. Scale-up of Pharmaceutical Spray Drying Using Scale-up Rules: A Review. *Int. J. Pharm.* **2019,** *562*, 271–292.

[14] Adali, M. B.; Barresi, A. A.; Boccardo, G.; Pisano, R. Spray Freeze-Drying as a Solution to Continuous Manufacturing of Pharmaceutical Products in Bulk. *Processes* **2020,** *8*(6), 709.

[15] Wanning, S.; Süverkrüp, R.; Lamprecht, A. Pharmaceutical Spray Freeze Drying. *Int. J. Pharm.* **2015,** *488*(1–2), 136–153.

[16] Ishwarya, S. P.; Anandharamakrishnan, C.; Stapley, A. G. F. Spray-Freeze-Drying: A Novel Process for the Drying of Foods and Bioproducts. *Trends Food Sci. Technol.* **2015,** *41*(2), 161–181.

[17] Wanning, S.; Süverkrüp, R.; Lamprecht, A. Impact of Excipient Choice on the Aerodynamic Performance of Inhalable Spray-Freeze-Dried Powders. *Int. J. Pharm.* **2020,** *586*, 119564.

[18] Williams III, R. O.; Johnston, K. P.; Young, T. J.; Rogers, T. L.; Barron, M. K.; Yu, Z.; Hu, J. Process for production of nanoparticles and microparticles by spray freezing into liquid. US Patent 6862890 B2, March 2005.

[19] Ryan, E.; Grice, J. E.; Roberts, M. S. Nanotechnology and Drug Delivery, Volume Two: Nano-Engineering Strategies and Nanomedicines against Severe Diseases, CRC Press, Boca Raton, FL, USA **2016,** 120.

[20] Williams III, R. O.; Watts, A. B.; Miller, D. A. Formulating Poorly Water Soluble Drugs, Springer, New York, **2012,** 533.

[21] Shapira, Y. Nano potent particles API freeze drying using organic solvent. ISLFD 2019 – 9th International Symposium on Lyophilization of Pharmaceuticals, September 2–6, 2019, Ghent, Belgium, **2019**.

[22]   Liang, W.; Chow, M. Y. T.; Chow, S. F.; Chan, H. K.; Kwok, P. C. L.; Lam, J. K. W. Using Two-Fluid Nozzle for Spray Freeze Drying to Produce Porous Powder Formulation of Naked SiRNA for Inhalation. *Int. J. Pharm.* **2018,** *552*(1–2), 67–75.

[23]   Lo, J. C. K.; Pan, H. W. Inhalable Protein Powder Prepared by Spray-Freeze-Drying Using Hydroxypropyl- β -Cyclodextrin as Excipient. *Pharmaceutics* **2021,** *13*(5), 1–15.

[24]   Pisano, R. Continuous Manufacturing of Lyophilized Products: Why and How to Make It Happen. *Am. Phar. Rev.* **2020,** 23, 20–22.

[25]   Topp, M. N.; Eisenklam, P. Industrial and medical uses of ultrasonic atomizers. *Ultrasonics* **1972,** *10*, 127-133.

[26]   Berger, H.; Mowbray, D.; Copeman, R.; Russell, R. Ultrasonic atomizing nozzle and method. U.S. Patent 0176017, 2007.

[27]   D'Addio, S. M.; Chan, J. G. Y.; Kwok, P. C. L.; Prud'Homme, R. K.; Chan, H. K. Constant Size, Variable Density Aerosol Particles by Ultrasonic Spray Freeze Drying. *Int. J. Pharm.* **2012,** *427*(2), 185–191.

[28]   Luz, P. P.; Pires, A. M.; Serra, O. A. A Low-Cost Ultrasonic Spray Dryer to Produce Spherical Microparticles from Polymeric Matrices. *Quim. Nova*. **2007,** *30*(7), 1744–1746.

[29]   Isleroglu, H.; Turker, I.; Tokatli, M.; Koc, B. Ultrasonic Spray-Freeze Drying of Partially Purified Microbial Transglutaminase. *Food Bioprod. Process.* **2018,** *111*, 153–164.

[30]   Ye, T.; Yu, J.; Luo, Q.; Wang, S.; Chan, H. K. Inhalable clarithromycin liposomal dry powders using ultrasonic spray freeze drying. *Powder Technol.* **2017,** 305, 63–70.

[31]   Liang, W.; Chan, A. Y. L.; Chow, M. Y. T.; Lo, F. F. K.; Qiu, Y.; Kwok, P. C. L.; Lam, J. K. W. Spray Freeze Drying of Small Nucleic Acids as Inhaled Powder for Pulmonary Delivery. Asian J. Pharm. Sci., 2018, 13 (2), 163–172.

[32]   Zhu, C.; Chen, J.; Yu, S.; Que, C.; Taylor, L. S.; Tan, W.; ... & Zhou, Q. T. Inhalable nanocomposite microparticles with enhanced dissolution and superior aerosol performance. *Molecular Pharmaceutics*, **2020,** 17(9), 3270–3280.

[33]   Patel, S. M.; Doen, T.; Pikal, M. J. Determination of End Point of Primary Drying in Freeze-Drying Process Control. *AAPS PharmSciTech*. **2010,** *11*(1), 73–84.

[34]   Horn, J.; Friess, W. Detection of Collapse and Crystallization of Saccharide, Protein, and Mannitol Formulations by Optical Fibers in Lyophilization. *Front. Chem.* **2018,** *6*, 1–9.

[35]   Her, L. M.; Nail, S. L. Measurement of glass transition temperatures of freeze-concentrated solutes by differential scanning calorimetry. *Pharm. Res.* **1994,** *11*, 54–59.

[36]   Adams, G. D.; Ramsay, J. R. Optimizing the lyophilization cycle and the consequences of collapse on the pharmaceutical acceptability of Erwinia L-asparaginase. *J. Pharm. Sci.* **1996,** *85*(12), 1301-1305.

[37]   Kim, A. I.; Akers, M. J.; Nail, S. L. The physical state of mannitol after freeze-drying: Effects of mannitol concentration, freezing rate, and a noncrystallizing cosolute. *J. Pharm. Sci.* **1998,** *87*(8), 931-935.

[38]   Kett, V. L.; Fitzpatrick, S.; Cooper, B.; Craig, D. Q. M. An investigation into the subambient behavior of aqueous mannitol solutions using differential scanning calorimetry, cold stage microscopy, and X-ray diffractometry. *J. Pharm. Sci.* **2003,** *92*(9), 1919-29.

[39]   Bubnik, Z.; Kadlec, P.; Bruhns, M. *Sugar technologists manual: Chemical and physical data for sugar manufacturers and users.* 8th edn. Verlag Dr. A. Bartens 1995; 134, 150-236.

[40]   Niwa, T.; Danjo, K. Design of Self-Dispersible Dry Nanosuspension through Wet Milling and Spray Freeze-Drying for Poorly Water-Soluble Drugs. *Eur. J. Pharm. Sci.* **2013,** *50*(3–4), 272–281.

[41]   Barron, M. K.; Young, T. J.; Johnston, K. P.; Williams, R. O. Investigation of Processing Parameters of Spray Freezing into Liquid to Prepare Polyethylene Glycol Polymeric Particles for Drug Delivery. *AAPS PharmSciTech*. **2003,** *4*(2), 1–13.

[42]   Schiffter, H.; Condliffe, J.; Vonhoff, S. Spray-Freeze-Drying of Nanosuspensions: The Manufacture of Insulin Particles for Needle-Free Ballistic

Powder Delivery. *J. R. Soc. Interface*, **2010,** *7*, 483–500.

[43] Sears, J.; Huang, K.; Ray, S.; Fairbanks, H. Effect of liquid properties on the production of aerosols with ultrasound. Ultrasonics Symposium Proceedings IEEE **1977,** 131-133.

[44] Kondo, M.; Niwa, T.; Okamoto, H.; Danjo, K. Particle Characterization of Poorly Water-Soluble Drugs Using a Spray Freeze Drying Technique. *Chem. Pharm. Bull.* **2009,** *57*(7), 657–662.

[45] Niwa, T.; Shimabara, H.; Kondo, M.; Danjo, K. Design of Porous Microparticles with Single-Micron Size by Novel Spray Freeze-Drying Technique Using Four-Fluid Nozzle. *Int. J. Pharm.* **2009,** *382*(1–2), 88–97.

[46] Kaialy, W.; Nokhodchi, A. Dry Powder Inhalers: Physicochemical and Aerosolization Properties of Several Size-Fractions of a Promising Alterative Carrier, Freeze-Dried Mannitol. *Eur. J. Pharm. Sci.* **2015,** *68*, 56–67.

[47] Tait, A.; Lee, J. G. M.; Williams, B. R.; Montague, G. A. Numerical Analysis of In-Flight Freezing Droplets: Application to Novel Particle Engineering Technology. *Food Bioprod. Process.* **2019,** *116*, 30–40.

List of Tables

Table 1. Results of particle size, as well as span value of the volume distribution, BET surface area and Karl-Fischer analysis were performed on the 3 formulations by varying the liquid flow rates.

Formulation (w/w)	Flow rate (mL/min)	Particle size		BET surface area (m²/g)	Moisture content (%)
		Mean diameter (μm)	Span* (±)		
5% Mannitol	1	14.99	1.54	7.58 ± 0.06	1.14 ± 0.01
	2.5	25.86	1.61	6.14 ± 0.09	1.25 ± 0.39
	5	32.48	2.04	7.53 ± 0.05	1.81 ± 0.24
	7.5	23.74	1.74	6.37 ± 0.04	0.94 ± 0.10
	10	65.96	1.05	5.55 ± 0.02	0.98 ± 0.05
5% Sucrose	1	14.55	1.34	0.23 ± 0.01	5.92 ± 0.09
	2.5	16.54	1.44	0.36 ± 0.01	6.14 ± 0.07
	5	21.88	2.03	1.37 ± 0.02	6.08 ± 0.24
	7.5	28.86	1.87	1.28 ± 0.02	5.58 ± 0.16
	10	30.36	1.80	2.31 ± 0.02	3.99 ± 0.13
40% Sucrose	1	30.90	1.10	1.47 ± 0.01	4.91 ± 0.58
	2.5	32.54	1.21	1.96 ± 0.02	4.42 ± 0.14
	5	40.03	1.28	4.55 ± 0.02	3.95 ± 0.15
	7.5	42.87	1.44	8.53 ± 0.04	3.30 ± 0.11
	10	47.63	1.81	8.97 ± 0.05	3.65 ± 0.04

* Span value calculated as (D90 - D10)/D50.

List of Figures

Figure 1. A schematic diagram of the SFD set-up.

Figure 2. DSC thermograms for (a) 5% (w/w) mannitol, (b) 5% (w/w) sucrose, (c) 40% (w/w) sucrose formulation.

Figure 3. SEM images of the particle surface for 5% (w/w) mannitol, 5% (w/w) sucrose, and 40% (w/w) sucrose, solutions sprayed at varying flow rates.

Figure 4. SEM images and particle size distribution histogram, with lognormal fitting curves, of spray freeze-dried powder in the case of the 5% (w/w) mannitol formulation and various values of the feed flow rate. The white bar corresponds to 100 μm.

Figure 5. SEM images and particle size distribution histogram, with lognormal fitting curves, of spray freeze-dried powder with 5% (w/w) sucrose formulation and varying flow rates. The white bar corresponds to 200 μm.

Figure 6. SEM images and particle size distribution histogram, with lognormal fitting curves, of spray freeze-dried powder with 40% (w/w) sucrose formulation and varying flow rates. The white bar corresponds to a width of 200 μm.

Figure 7. XRD pattern for the powders produced from 5% (w/w) mannitol solution at various flow rates. The labels identify the most representative peaks for the anhydrous β (♦) and d (●) polymorphs and for the (*) hemihydrate.

Figure 8. Onset-Offset times for the freeze-drying cycles, (a) 5% (w/w) mannitol sprayed at flow rates of 1 mL/min (red continuous line) and 10 mL/min (red dashed line), (b) 5% (w/w) sucrose sprayed at flow rates of 1 mL/min (red continuous line) and 10 mL/min (red dashed line), (c) 40% (w/w) sucrose sprayed at flow rates of 1 mL/min (red continuous line) and 10 mL/min (red dashed line). Note that the axis scales of each of the figures are different.
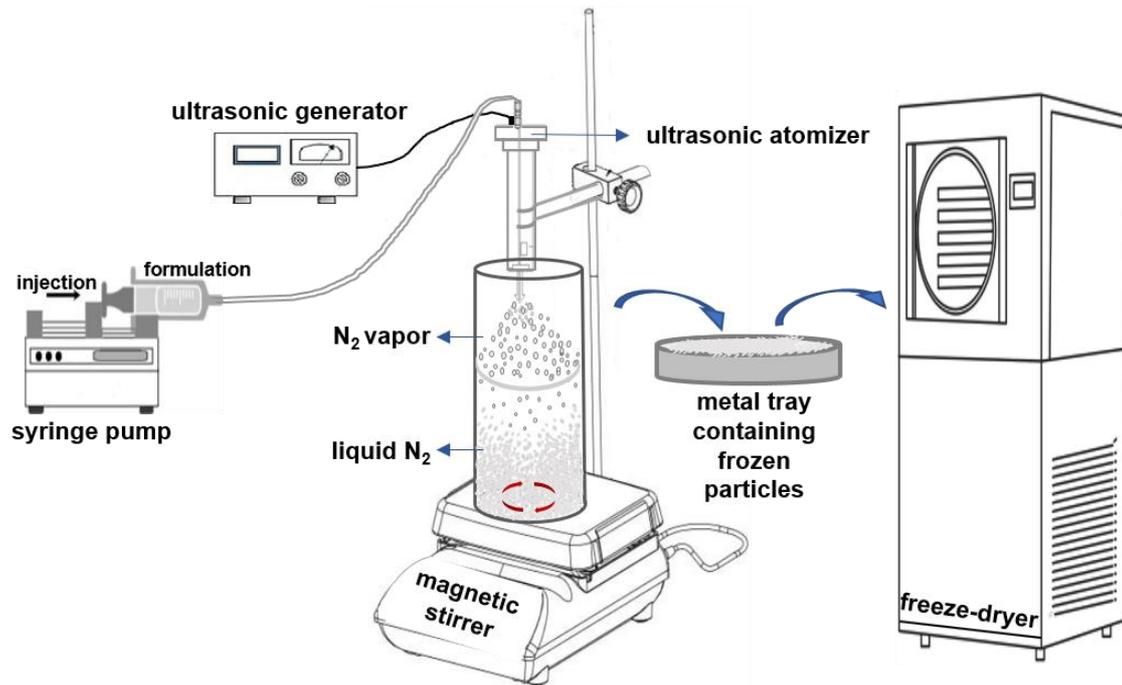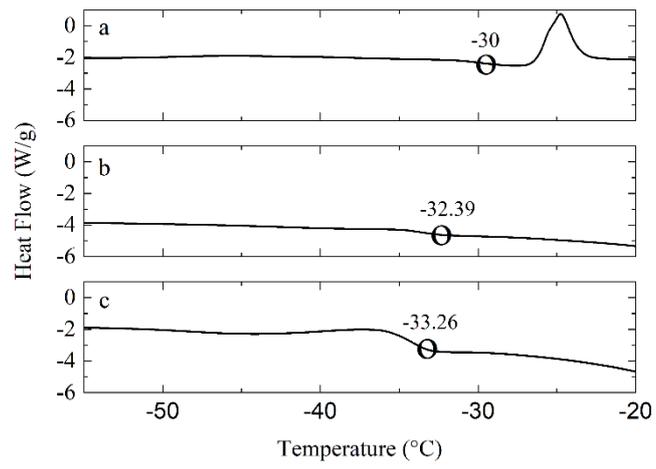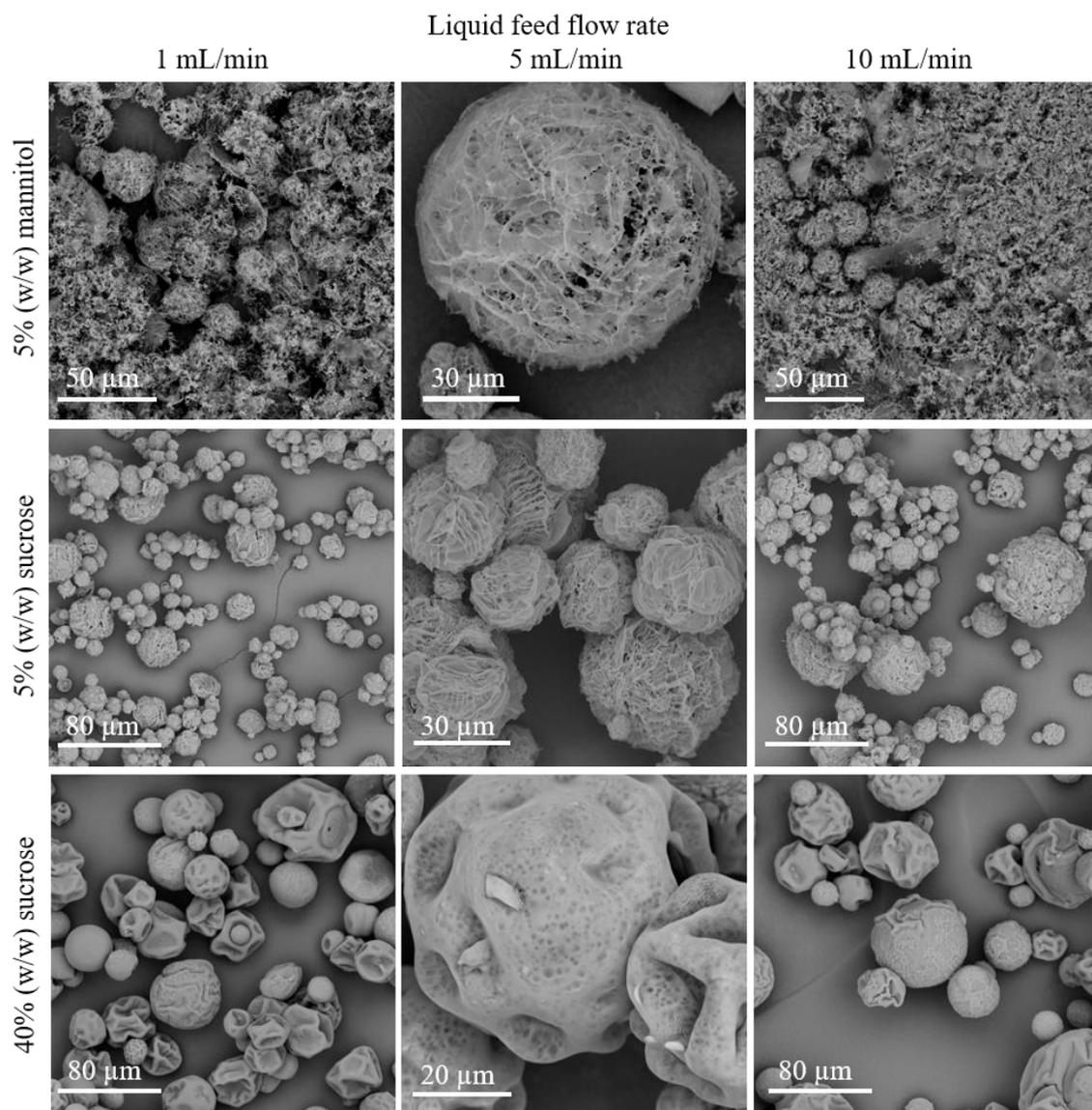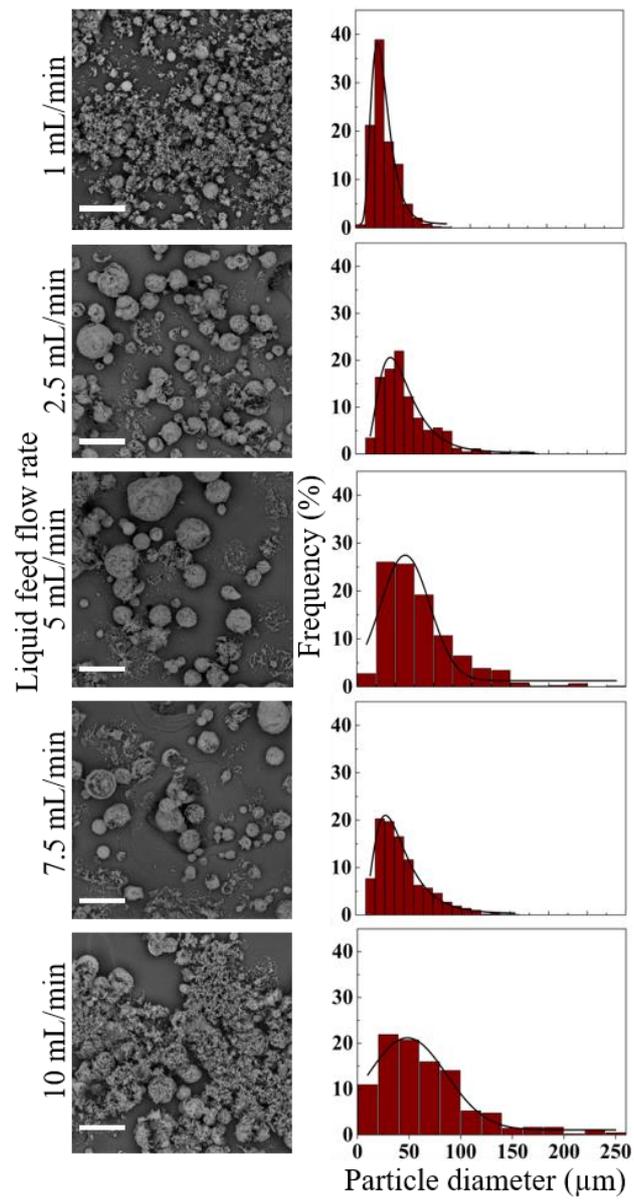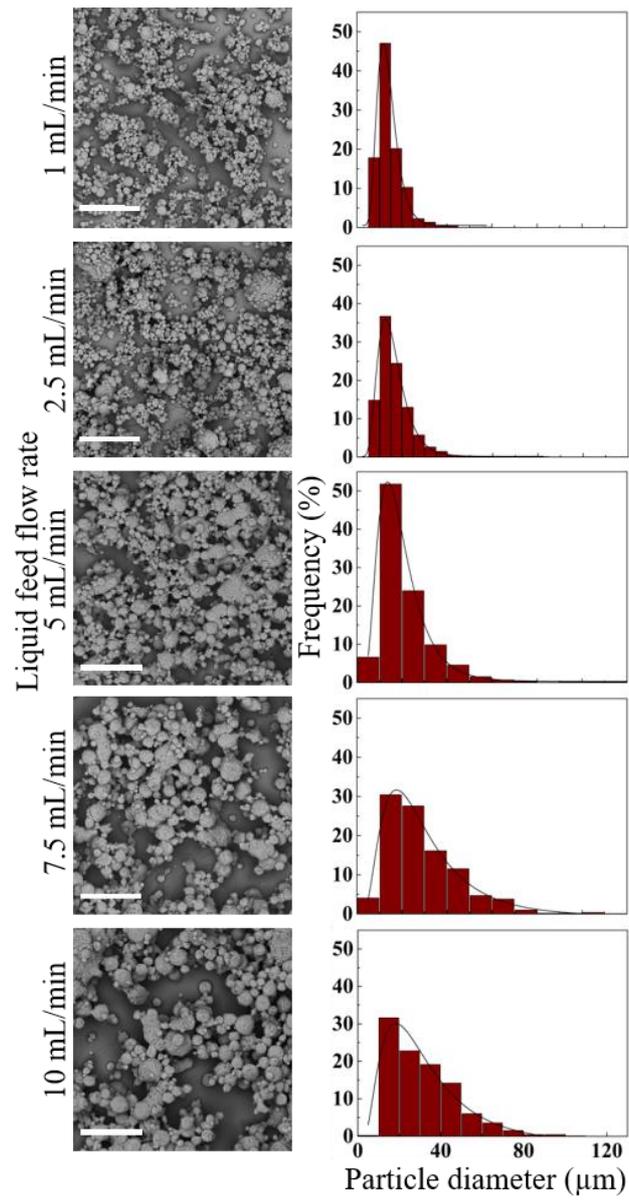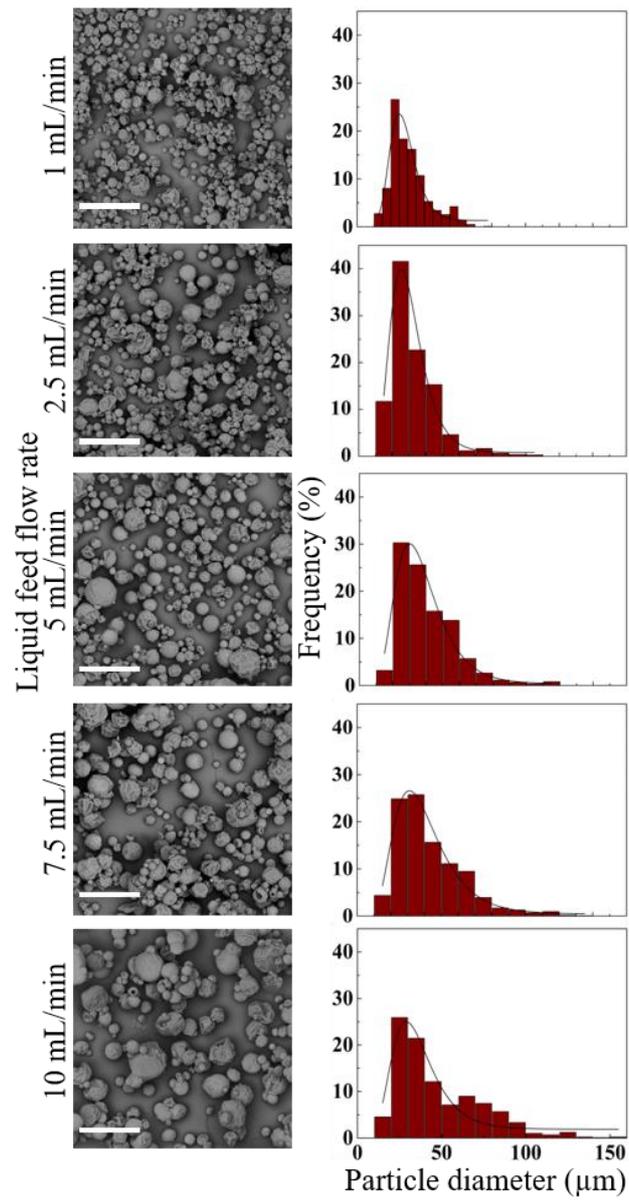
Figure 1

Figure 2

Figure 3

Figure 4

Figure 5

Figure 6

Figure 7

Figure 8